EurJIC
European Journal of Inorganic Chemistry

Research Article
doi.org/10.1002/ejic.202400292

Chemistry Europe
European Chemical Societies Publishing

www.eurjic.org

Reduction of Exfoliated MoS_2 Nanosheets Yields the Semi-Conducting 2H-polymorph Rather Than the Metallic 1T-polymorph

Aleksandra M. Krajewska,[a] Aislan Esmeraldo Paiva,[a] Michael Morris,[a] and Aidan R. McDonald*[a]

Delaminated two-dimensional (2D) transition metal dichalcogenides (TMDs) have attracted significant attention due to their potential application in electronics, catalysis, and biomedical devices. Chemical derivation of TMDs often relies on the generation of a metallic polymorph (1T) which is unsuitable for such applications. We explored the reactivity of the semi-conducting polymorph (2H) of pre-exfoliated MoS_2 nanosheets (as a model TMD). Pristine liquid exfoliated 2H-MoS_2 was reacted with $NaBH_4$. A novel reduced two-dimensional TMD, r-2H-MoS_2, was identified as evidenced by electronic absorption, XPS, photoluminescence, DRIFT, and Raman spectroscopies, and cyclic voltammetry. The material demonstrated a full preservation of the semi-conducting phase rather than conversion to the metallic 1T-nanomaterial that is commonly observed in the chemical derivation/exfoliation of TMDs.

Introduction

Exfoliated two-dimensional transition metal dichalcogenides (TMDs) have demonstrated potential for applications in a variety of fields, as long as facile exfoliation and chemical derivation can be achieved.[1] MoS_2, as the model TMD, has attracted considerable focus due to its natural availability/abundance and potential applications in electronic devices, photonic devices, catalyzed hydrogen evolution (HER), energy storage, and sensor materials.[2] Importantly, the two most-commonly identified polymorphs are the 2H-phase (trigonal prismatic at Mo) and the 1T-phase (octahedral at Mo).[2d,3] Monolayers of 2H-MoS_2 are semi-conducting and tend to be the more interesting material from a device perspective. In contrast, 1T-MoS_2 is metallic and only in the HER reaction does it display improved properties with respect to the 2H phase.

Two-dimensional MoS_2 can be accessed through mechanical methods, hydrothermal synthesis, chemical vapour deposition (CVD) methods, chemical and electrochemical exfoliation, and liquid-phase exfoliation.[1] The latter two methods are most-commonly employed to obtain reasonable quantities of exfoliated materials. The chemical exfoliation methods involve a reaction between bulk 2H-MoS_2 and n-butyllithium (^{n}BuLi, Scheme 1), yielding the reduced intercalated product Li_x[1T-MoS_2]$^{x-}$.[4] Other Li-reductants ($LiBH_4$ or *tert*-butyllithium, ^{t}BuLi) yield the same outcome.[5] The intercalation of Na^+ or K^+ ions could also be achieved if the expansion of the lattice was first aided by the insertion of smaller molecules like ammonia or hydrazine.[6] $NaBH_4$ reduction of bulk MoS_2 yielded highly defective products *and* the 1T-phase.[7] Subsequent reaction with H_2O causes delamination and hydrogen evolution, yielding monolayers of so-called chemically exfoliated MoS_2. Critically, chemical exfoliation *always* yields the 1T-phase, and always results in residual charge at the surface of the nanomaterial, alongside a highly defective material. This residual charge renders 1T-MoS_2 highly conductive, an effective HER catalyst, dispersable in polar solvents, and readily functionalized. In contrast, 2H-MoS_2 (obtained through hydrothermal synthesis, CVD, or liquid-phase exfoliation) is chemically inert, poorly dispersed, and difficult to derivatize. Semi-conducting 2H-MoS_2, while displaying many fascinating properties, is thus difficult to handle, difficult to obtain in high yields, and difficult to derivatize.

The reactivity of 2H-MoS_2 with reducing agents has been explored mostly in the context of exfoliation and phase transition to the 1T-polymorph (Scheme 1). As described, Li^+, Na^+, K^+ ions readily intercalate upon reaction with bulk 2H-MoS_2 *in the presence of a reductant*, with the intercalated product always found in the 1T polytype. The metal intercalated compounds were subsequently reacted with H_2O, resulting in reoxidation and exfoliation of MoS_2 and loss of H_2 and MOH. The production of H_2 bubbles is believed to cause delamination of the nanosheets. Critically, the reoxidation with H_2O did *not* lead to the transformation from the 1T-phase to the thermodynamically stable and semi-conducting 2H-phase. Thus, chemical methods to derivatize MoS_2 yield the 1T-polymorph. Interestingly, to the best of our knowledge, no attention has been paid to the reduction of pre-exfoliated 2H-MoS_2. Herein, we explore the reaction of liquid-exfoliated 2H-MoS_2 with a reducing agent

[a] A. M. Krajewska, A. E. Paiva, M. Morris, A. R. McDonald
CRANN/AMBER Nanoscience Institute and School of Chemistry, Trinity College Dublin, The University of Dublin, College Green, 2 Dublin, Ireland
E-mail: aidan.mcdonald@tcd.ie

Supporting information for this article is available on the WWW under https://doi.org/10.1002/ejic.202400292

Research Article
doi.org/10.1002/ejic.202400292

Chemistry Europe
European Chemical Societies Publishing

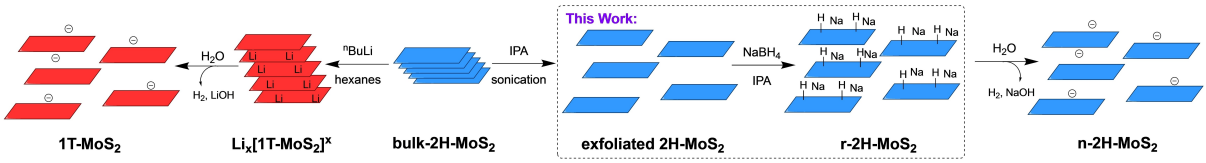

Scheme 1. Methods for preparation of exfoliated 1T- (red) and 2H-polymorphs (blue) of MoS_2 and their derivatives.

($NaBH_4$) demonstrating the formation of a reduced form of MoS_2 that maintains the 2H polymorph.

Results and Discussion

Liquid-phase exfoliated 2H-MoS_2 in 2-propanol (IPA) was prepared according to methods previously reported by us and others (Scheme 1).[8] As in our earlier studies, the obtained flakes displayed a mean thickness of 10 nanosheets and the concentration in IPA was ~0.4 g/L. We employ materials of this thickness and concentration because it is challenging to obtain sufficient quantities of material for further studies when the liquid exfoliation process is extended to yield mono-layered material. This pristine 2H-MoS_2 was subsequently reacted with $NaBH_4$ (30 equiv.) in IPA for 24 h at room temperature under magnetic stirring (see supporting information file for details). The resulting sediment was subjected to high-speed centrifugation. To isolate the sediment, it was filtered onto a 0.2 μm nylon filter membrane (Figure 1). The obtained solid had visibly different properties compared to pristine 2H-MoS_2 or n-2H-MoS_2. Upon filtration, the material did not form a film on the membrane, but rather became brittle and started to crack. Interestingly, the addition of a single drop of H_2O onto the membrane containing the sediment, resulted in the generation of the characteristic n-2H-MoS_2 film and an evolution of a gas was observed (Figure 1). In our previous report on the preparation of n-2H-MoS_2,[8b] reacting the obtained sediment with H_2O lead to gas evolution and the formation of n-2H-MoS_2.

Rather than add H_2O, herein we isolated and characterized the sediment formed after the initial reaction with $NaBH_4$. Thus, initial visual observations of the sediment suggested it was a novel material, leading us to define it as a reduced form of MoS_2, namely r-2H-MoS_2.

r-2H-MoS_2 was collected from the membrane promptly after filtration and was dried under reduced pressure. The material was stored under an inert atmosphere to minimize exposure to atmospheric moisture (given the observation that it was reactive towards H_2O). All solid-state characterizations were performed on this as-isolated material. For solution-phase characterization, r-2H-MoS_2 was re-dispersed in IPA or alternative solvents. It is worth noting that r-2H-MoS_2 did not react with IPA (in contrast to the immediate reaction with H_2O).

The electronic absorption spectrum of r-2H-MoS_2 in IPA displayed the presence of the characteristic 2H-MoS_2 transitions λ_{A-D} (Figure 2, r-2H-MoS_2: $\lambda_A = 685$, $\lambda_B = 625$, $\lambda_C = 490$, and $\lambda_D = 406$ nm; pristine 2H-MoS_2: $\lambda_A = 674$, $\lambda_B = 614$, $\lambda_C = 457$, and $\lambda_D = 406$ nm).[9] Critically, no new transitions were observed in the UV region, where the 1T-MoS_2 polymorph typically displayed absorption bands ($\lambda = 260$, 300 nm).[3a] Both of those observations indicated that upon reaction with $NaBH_4$ no change in the polymorph had occurred and that the novel material preserved the 2H phase. It was also noted that the transitions observed in r-2H-MoS_2 were red-shifted with respect to pristine 2H-MoS_2: λ_A and λ_B by 10 nm and λ_C by 30 nm. Moreover, a significant baseline shift was observed in the spectrum compared to

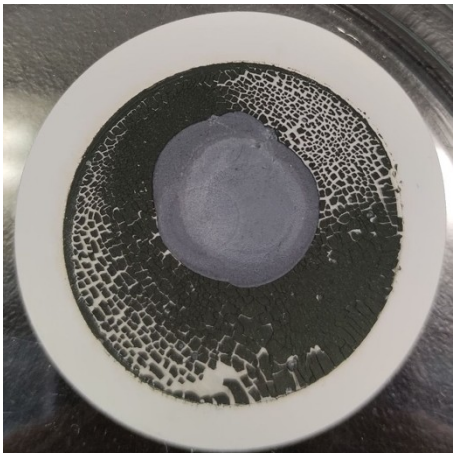

Figure 1. Photograph of the sediment on a nylon membrane. The darker, apparently quite brittle areas, represent r-2H-MoS_2. The grey area is the n-2H-MoS_2 film that has formed after the addition of a drop of H_2O.

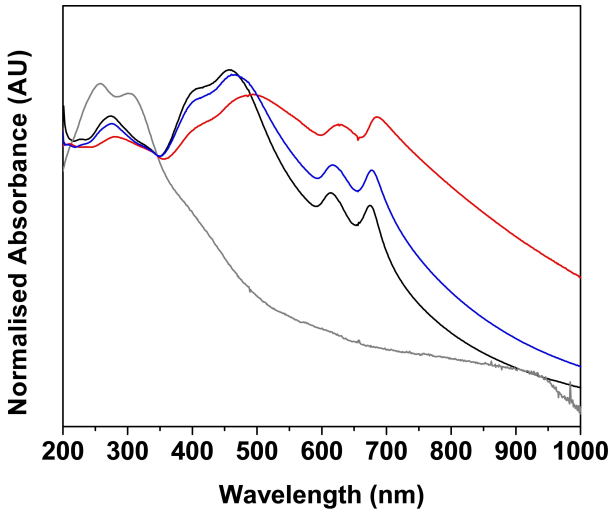

Figure 2. Electronic absorption spectra of r-2H-MoS_2 in IPA (red), n-2H-MoS_2 in IPA (blue), pristine 2H-MoS_2 in IPA (black), and 1T-MoS_2 in H_2O (grey). All spectra were normalized at $\lambda = 345$ nm.

Research Article
doi.org/10.1002/ejic.202400292

pristine 2H-MoS_2 collected in the same solvent. Such a baseline shift is normally attributed to poorer dispersibility in the solvent.[8–9] This demonstrated that despite the preservation of the same phase, a significant change in the surface properties of the material had occurred and that r-2H-MoS_2 was not able to form a stable dispersion in IPA, likely due to agglomeration of the particles. In comparison to n-2H-MoS_2, r-2H-MoS_2 and pristine 2H-MoS_2 appear to be two extremes, where n-2H-MoS_2 represents the middle-ground. This is consistent with our analysis of n-2H-MoS2 which displayed a partial build-up of charge, however, not to the degree measured in r-2H-MoS_2 as described below. Electronic absorption spectroscopy thus indicated that r-2H-MoS_2 was a novel form of the 2H-polymorph of MoS_2, displaying features typical of the semiconducting 2H phase and no indications of the metallic 1T phase.

The photoluminescence spectrum of r-2H-MoS_2 displayed one emission peak centered at $\lambda = 705$ nm (Figure 3). This is within the energy range of the direct bandgap observed in 2H-MoS_2 ($\lambda = 660$-710 nm),[3b] indicating the preservation of the semiconducting phase in r-2H-MoS_2. The energy of emission was 20 nm (0.05 eV) red-shifted with respect to pristine 2H-MoS_2 ($\lambda = 685$ nm). This decrease in energy suggested the presence of additional electron density and an effective n-doping in r-2H-MoS_2. Interestingly, the emission was observed at the same wavelength as the photoluminescence in n-2H-MoS_2 ($\lambda = 705$ nm, Figure S1). The fact that the emission of r-2H-MoS_2 was observed at the same energy as the emission from n-2H-MoS_2 demonstrated that the shift in the energy is likely due to the formation of trions and can be linked to the excitons interacting with the excess of electrons in both samples.[10]

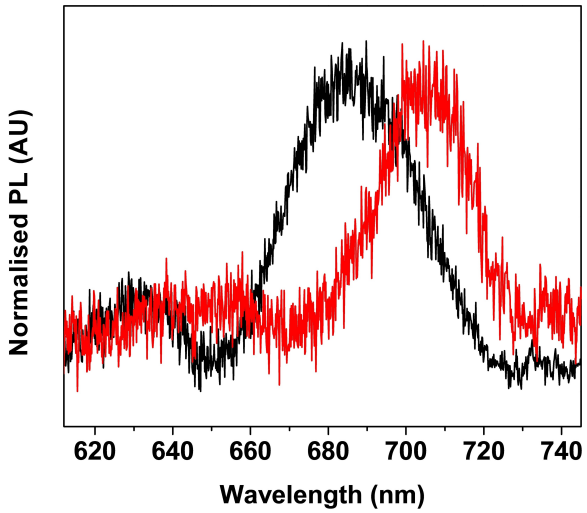

Figure 3. Photoluminescence spectra of r-2H-MoS_2 (red) and pristine 2H-MoS_2 (black).

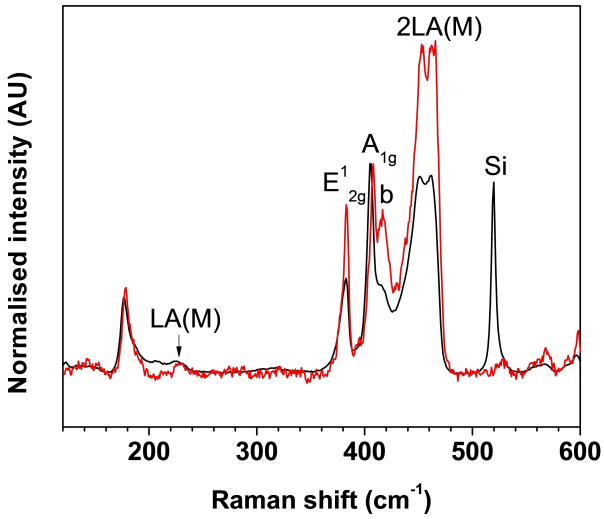

Figure 4. Raman spectra of r-2H-MoS_2 (red) and pristine 2H-MoS_2 (black). Spectra were normalized to the A_{1g} peak intensity.

Raman analyses of r-2H-MoS_2 showed resonances that could be attributed to the E^1_{2g}, A_{1g}, and 2LA(M) modes ($\nu = 384$, 408, and 458 cm^{-1}, respectively), previously identified as characteristic of 2H-MoS_2 (Figure 4).[11] Importantly, the r-2H-MoS_2 spectrum displayed a stark increase in the 2LA(M) mode intensity in comparison to pristine 2H-MoS_2 (2LA(M):$A_{1g} = 1.34$ and 0.98, respectively). The 2LA(M) mode is especially sensitive to any chemical or physical changes in the sample.[12] It is a strong indicator of chemical changes on the surface of 2H-MoS_2, suggesting that r-2H-MoS_2 was chemically modified with respect to pristine 2H-MoS_2. One explanation for the increase in the 2LA(M) mode intensity could be an increase in the defect density.[13] However, more reliable observations correlated with defects were associated with the LA(M) mode ($\nu = 227$ cm^{-1}). Here, a weak LA(M) mode was detected in the spectrum of r-2H-MoS_2, however, it displayed the same intensity in pristine 2H-MoS_2. This indicated that there was no significant increase in the defect density in r-2H-MoS_2. The intensity of the 2LA(M) was also suggested to increase when the laser excitation wavelength approached the energy of the photoluminescence emission.[14] However, the photoluminescence emission for r-2H-MoS_2 was at higher wavelength ($\lambda = 705$ nm) than pristine 2H-MoS_2 ($\lambda = 685$ nm), pushing it further away from the 633 nm excitation energy, ruling this phenomenon out. Thus, we postulate that the increase in the 2LA(M) mode intensity is plausibly caused by the increase in the electron density in the material, which could be linked to the accumulation of the higher electron density in the valence band. The slight offset in the A_{1g} energy was ascribed to the reduction of the material, something that was previously observed for hot-electron doping of MoS_2.[15] Finally, J peaks that are normally characteristic of the 1T-MoS_2 polymorph ($\nu_{J1-J3} = 156$, 226, 333 cm^{-1}),[16] were not present in r-2H-MoS_2, supporting the retention of the 2H polymorph. Overall, Raman analysis showed r-2H-MoS_2 to be a chemically modified form of 2H-MoS_2, with indications that it was reduced with respect to pristine 2H-MoS_2.

A survey X-ray photoelectron spectroscopy (XPS) analysis of r-2H-MoS_2 displayed the presence of Mo, S, Na, B, C, and O in the material (Figure S2). The ratio of Mo:S atoms (1:1.7) was within the range expected for 2H-MoS_2 and any differences are likely due to preferential alignment of the samples.[9a] The Na:B ratio was found to equal 2.2:1, even though these elements were introduced in a 1:1 ratio in the form of $NaBH_4$. This suggested that the reaction between 2H-MoS_2 and $NaBH_4$

Research Article
doi.org/10.1002/ejic.202400292

resulted in the formation of a collected product that retained Na while some B-containing products were lost (presumably during centrifugation/filtration). The presence of O signalled that the product contained IPA, water, and/or oxygenated products.

The analysis of the S 2p and Mo 3d core level XPS spectra revealed significant changes consistent with an increased electron density in r-2H-MoS_2 (Figure 5). The binding energy maximum shifted by 0.8 eV to lower energy for both elements. The S 2p region displayed two peaks at 161.7 and 162.9 eV (S 2p 3/2 and S 2p $^1/_2$, respectively) in r-2H-MoS_2 compared to 162.5 and 163.7 eV in pristine 2H-MoS_2. Similarly, the Mo 3d components were found at 228.9 and 232.1 eV (Mo 3d 5/2 and Mo 3d 3/2, respectively) in r-2H-MoS_2, compared to 229.7 and 232.9 eV in pristine 2H-MoS_2. This shift in the binding energy of the core orbitals demonstrated a significant increase in the electron density in the material, indicating that r-2H-MoS_2 represented a reduced form of 2H-MoS_2. The binding energy has been observed to shift when comparing the phase transformation from the 2H to 1T-polymorph of MoS_2.[3a,17] This shift is usually between 0.8–0.9 eV and in many reports is used as a confirmation of the phase transition from the 2H to 1T polymorph. However, it should be noted that the 1T-phase always suffers from accumulated negative charge, because of the method of preparation - we contend that the negative shift is simply a designation of charge accumulation rather than phase change, which is supported by observations elsewhere exploring the redox chemistry of MoS_2.[18] All other spectroscopic analyses of r-2H-MoS_2 demonstrate that it retains the 2H polymorph and that the 1T-polymorph was absent. Finally, the XPS spectra for both elements displayed peak broadening by 0.4 eV and 0.3 eV, respectively, as measured by the full width at half maximum (FWHM) against pristine 2H-MoS_2. This suggests that there is likely some uncharged 2H-MoS_2 in the sample causing the peak broadening, as observed previously for studies on chemical changes at the surface of MoS_2.[8a,12a,19]

The B 1s core level spectrum of r-2H-MoS_2 displayed a one-component feature localized at 192.0 eV (Figure S3). $NaBH_4$ would be expected at a lower energy of 188.7 eV, indicating that all $NaBH_4$ had been consumed and that the new species was likely an oxidized form of B.[20] Boron oxides or boric acids are generally observed at a higher energy, approximately ~193.0–193.3 eV. Borates, in contrast are generally observed in the region of 191.8–192.0 eV, leading us to conclude that the B in r-2H-MoS_2 was a borate. The Na 1s core level spectrum also displayed a one-component feature at 171.3 eV (Figure S4). The position of the peak did not reveal any details about the nature of the Na adduct, as any differences in the binding energy of Na in varying chemical environments are rather modest.[21] The analysis of the O 1s core level spectrum displayed a two-component fit (Figure S3), with binding energies = 531.5 eV and 535.9 eV (ratio 1:0.45). The high energy component was identified as H_2O,[22] whereas the peak at 531.5 eV was consistent with borate.[23] We conclude, based on the B and O core level spectra that $NaBH_4$ was converted to $Na_2B_4O_5(OH)_4{}^{\bullet}xH_2O$ (sodium borate hydrate) in the preparation of r-2H-MoS_2. Importantly, the survey spectrum indicated a Na:B ratio of 2:1, inconsistent with the ratio in $Na_2B_4O_5(OH)_4{}^{\bullet}xH_2O$. We surmise that the remaining Na was present in the r-2H-MoS_2 sample acting to balance the charge at the surface of r-2H-MoS_2, which might better be formulated as $Na_x[(H)_x2H\text{-}MoS_2]$.

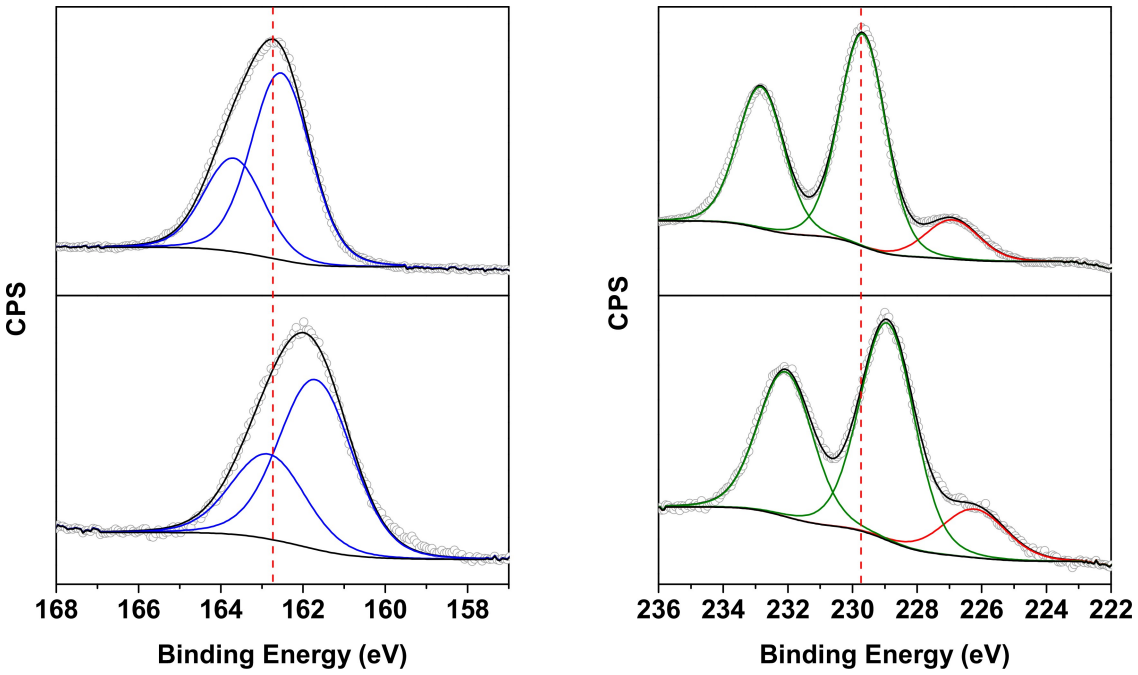

Figure 5. Core level XPS spectra of S 2p (left) and Mo 3d (right) for 2H-MoS_2 (top) and r-2H-MoS_2 (bottom). Color code: experimental data (grey circles), fits of: S 2p (blue), S 2 s (red), Mo 3d (green), summed simulation fit (black). The red dashed lines centred at 162.8 and 229.7 eV to emphasize shift upon generation of r-2H-MoS_2. CPS stands for counts per second.

Research Article
doi.org/10.1002/ejic.202400292

Diffuse reflectance infra-red Fourier transform (DRIFT) analysis of r-2H-MoS_2 displayed the characteristic Mo–S stretching mode identified in MoS_2 located at $\nu = 384\ cm^{-1}$ (Figure 6).[24] However, the other features normally associated with pristine 2H-MoS_2 were masked by new broad features. In particular, new resonances at $\nu = 3330$, 1360, and 980 cm^{-1} were identified which could be attributed to sodium borates ($Na_2B_4O_5(OH)_4{\bullet}xH_2O$, Table S1).[25]

Importantly, r-2H-MoS_2 displayed new features at $\nu = 1775\ cm^{-1}$ and 2290 cm^{-1} which could not be ascribed to either the $Na_2B_4O_5(OH)_4{\bullet}8H_2O$ or pristine 2H-MoS_2. We postulate that the $\nu = 1775\ cm^{-1}$ peak corresponds to a ν_{Mo-H} stretch, which is in good agreement with literature reports of such modes found in MoS_2,[26] but was ~40–170 cm^{-1} lower in energy in comparison to the Mo–H bonds reported in molecular systems.[27] Similarly, we assigned the $\nu = 2290\ cm^{-1}$ feature to ν_{S-H}, which are typically found in the $\nu = 2500–2600\ cm^{-1}$ range for organic thiols, while for metallo-hydrosulfides they are generally found between $\nu = 2450–2650\ cm^{-1}$, but can be as low as $\nu = 2150\ cm^{-1}$.[9a,28] To probe these features further, we prepared r-2H-MoS_2 with $NaBD_4$. The DRIFT spectrum of r-2H-MoS_2 obtained with the deuterated reducing agent displayed the Mo–S stretching mode at $\nu = 384\ cm^{-1}$ (Figure 6), together with all the vibrations previously ascribed to $Na_2B_4O_5(OH){\bullet}xH_2O$. The features at $\nu_{Mo-H} = 1775\ cm^{-1}$ and $\nu_{S-H} = 2290\ cm^{-1}$ were expected to shift to $\nu = 1262$ and 1644 cm^{-1} for ν_{Mo-D} and ν_{S-D}, respectively. We noted a change in the shape of the band at ν~1630 cm^{-1} which we assign to contributions from ν_{S-D} (Figure S5). We believe the ν_{Mo-D} is masked by other features. Despite this, the disappearance of the Mo–H and S–H bonds as well as the visible contribution of S–D vibration into the r-2H-MoS_2 spectrum have provided further evidence for the hydride attachment from reaction with $NaBH_4$ *and* 2H-MoS_2 reduction during the formation of r-2H-MoS_2. Infra-red analysis thus provides strong evidence that r-2H-MoS_2 is a reduced form of MoS_2 that has incorporated hydride through the formation of Mo–H or S–H bonds.

Thermogravimetric analysis (TGA) of r-2H-MoS_2 displayed a thermogravimetric trace different to that of pristine 2H-MoS_2 (Figure S6). For r-2H-MoS_2 there was a 16% overall mass loss between 100–800 °C, compared to the just 2% loss for the pristine material. r-2H-MoS_2 underwent three mass loss events: 100–300 °C (10%), 450–600 °C (2%), and 670–800 °C (4%). The first two mass loss events can be ascribed to the decomposition of $Na_2B_4O_5(OH){\bullet}xH_2O$.[29] The assignment of the third event was more challenging to assess, hence TGA was coupled with FT-IR to aid the identification of gaseous molecules desorbing (Figure S7). No new vibrations were detected until 720 °C was reached when the formation of a resonance at $\nu = 1350\ cm^{-1}$ was observed, corresponding well with the temperature of the third mass loss event. This was ascribed to ν_{as} of SO_2,[30] which indicated the decomposition of the r-2H-MoS_2 lattice. Importantly pristine 2H-MoS_2 did not display the same mass loss. This suggests that r-2H-MoS_2 has a different, less thermally stable, chemical composition than pristine 2H-MoS_2. TGA thus confirmed the presence of $Na_2B_4O_5(OH)_4{\bullet}xH_2O$ in r-2H-MoS_2 as well as providing indications that the MoS_2 was chemically modified, consistent with other observations.

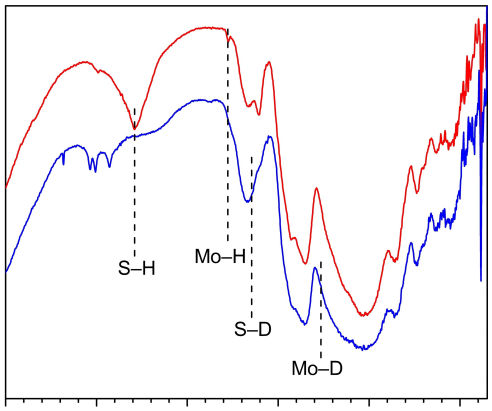

Figure 6. DRIFT spectra of r-2H-MoS_2 synthesized with $NaBH_4$ (red trace) and $NaBD_4$ (blue trace).

With powder X-ray diffraction (pXRD) measurements it was possible to discriminate all the characteristic reflections of the 2H-phase in r-2H-MoS_2 (Figure S8), with a perfect overlap with those observed in the pristine 2H-MoS_2 pattern. At the same time, no broadening of the reflections was observed indicating that there was no loss of the crystallinity in favor of the 1T or an amorphous phase nor a reduction in thickness.[31] Importantly, there were no new peaks present in the diffraction pattern, especially at $^{\circ}2\theta$ lower than the 002 reflection. We surmise that the reason that we do not observe borate by pXRD is that it is likely amorphous, and the degree of hydration in borate was not clear. This indicated that there was no Na-ion intercalated between the layers of the intermediate species.[32]

The zeta-potential of r-2H-MoS_2 in IPA was examined to further investigate the surface properties of the material. However, during the measurement, the particles were found to flocculate becoming increasingly large upon the application of the voltage, making any data collected unreliable - the measured data was extremely broad and poorly resolved (Figure S9). This prevented us from assessing the charge on the surface using zeta-potential measurements.

To analyze the redox properties of r-2H-MoS_2, the material was characterized with cyclic voltammetry (CV). A three-electrode set-up in $^{n}Bu_4NPF_6$ (CH_3CN, 0.1 M) was used. r-2H-MoS_2 was drop-cast onto a glassy carbon and the CV was recorded (Figure S10). The r-2H-MoS_2 voltammogram displayed a chemically irreversible oxidation wave (E = 0.13 V), which was absent in pristine 2H-MoS_2. The presence of this new oxidation event indicated that r-2H-MoS_2 was present in a reduced form that was oxidized under the CV conditions. Importantly, this oxidation event was absent in the voltammograms of 2H-MoS_2 and 1T-MoS_2,[4] signifying the difference in the oxidation state observed in r-2H-MoS_2. Overall, CV demonstrated that r-2H-MoS_2 was present in a reduced form.

Negative charge accumulation has been shown to affect the surface properties of n-2H-MoS_2 and 1T-MoS_2.[17] We previously demonstrated that the dispersibility of these charged MoS_2 species could be correlated with the relative permittivity expression of the solvents. The negative charge detected in r-

Research Article
doi.org/10.1002/ejic.202400292

2H-MoS_2 was more substantial according to XPS, indicating the reduction of the material. r-2H-MoS_2 was re-dispersed in IPA, dimethylsulfoxide (DMSO), CH_3CN, acetone, toluene, N-methylpyrolidinone (NMP), and diethylether Et_2O (Figure S11, note that H_2O was not used as that would have yielded the formation of n-2H-MoS_2). r-2H-MoS_2 displayed a relatively poor dispersibility in all solvents tested. The material visibly flocculated within 30 minutes in all cases. Electronic absorption spectra revealed some differences in the relative dispersibility of r-2H-MoS_2 (Figure S11): very poor dispersibility was observed in acetone, CH_3CN, toluene and Et_2O as indicated by a high baseline shift. The baseline absorption was the lowest in IPA, DMSO, and NMP. A poor correlation between the dispersibility and the relative permittivity expression was observed.[17] This would suggest that the nature of the n-doping in r-2H-MoS_2 is different *and* has a different effect on the surface properties of the material than we observed in the cases of n-2H-MoS_2 and 1T-MoS_2.

Mechanism of r- and n-2H-MoS_2 Formation

When r-2H-MoS_2 was reacted with H_2O, a visible change, from a brittle solid to a solid that was collected as a film, was observed alongside gas evolution. We surmised that the gas evolved was H_2 and have characterized the obtained product as n-2H-MoS_2. This sequence mirrors the observations made in the preparation of 1T-MoS_2:[2d,3] reaction of bulk 2H-MoS_2 with a reductant, ^{n}BuLi, yielded Li_x[1T-MoS_2]^x followed by oxidative quenching with H_2O resulting in the evolution of a gas (H_2) which caused delamination yielding monolayers of so-called 'chemically exfoliated' 1T-MoS_2. The difference for r-2H-MoS_2 was that we employed $NaBH_4$ on *pre-exfoliated* 2H-MoS_2 and obtained the reduced form of the 2H polymorph, Na_x[$(H)_x$2H-MoS_2], which reacted with water to give n-2H-MoS_2. It thus appears that $NaBH_4$ reduction of pre-exfoliated 2H-MoS_2 yielded a reduced form of the 2H-polymorph without isomerization to the 1T (Scheme 2).

We postulate that in the reaction of pristine 2H-MoS_2 with $NaBH_4$, H^- performs a nucleophilic attack at an Mo exposed site (such as an S-vacancy). This results in the formation of a new Mo–H (as identified by DRIFT analysis) bond and an overall reduction of 2H-MoS_2 to r-2H-MoS_2 (Scheme 2). It is also possible that H^- attack occurred at a sulfide or that Mo–H formed and the H-atom transferred to an S-site, yielding the DRIFT observed S–H moiety. The negative charge introduced into the material with the H^- transfer is balanced by adsorbed Na^+ cations. In the presence of atmospheric oxygen and/or H_2O, the BH_3 that was formed after the H^- donation from $NaBH_4$, presumably underwent a multi-step conversion to the identified $Na_2B_4O_5(OH)_4{\bullet}xH_2O$. We concluded that the mode of reduction by $NaBH_4$ yielded only surface-altered 2H-MoS_2, with no evidence for Na intercalation. This contrasts to the reaction between bulk 2H-MoS_2 and ^{n}BuLi, which resulted in Li^+ intercalation and a change in electronic structure and thus polymorph (trigonal prismatic at Mo to octahedral at Mo).

Conclusions

The activation of pre-exfoliated pristine 2H-MoS_2 was explored through its reaction with a reductant, $NaBH_4$. A novel two-dimensional nanomaterial, r-2H-MoS_2, was identified as a reduced form of MoS_2, as indicated by an XPS peak shift to lower binding energy by 0.8 eV compared to pristine 2H-MoS_2 in both the S 2p and Mo 3d core level spectra. The reduction was further indicated by CV, photoluminescence, DRIFT, and Raman spectroscopies. The material demonstrated a full preservation of the trigonal prismatic geometry at Mo in 2H-MoS_2 as indicated by electronic absorption spectroscopy, pXRD, Raman spectroscopy, and photoluminescence measurements. r-2H-MoS_2 reacted with H_2O resulting in the formation of a negatively charged form of 2H-MoS_2 (n-2H-MoS_2). This sequence mirrors the common preparation of the delaminated metallic phase 1T-MoS_2, where reaction of bulk 2H-MoS_2 with a reductant (^{n}BuLi) yielded Li_x[1T-MoS_2]^x which was quenched with H_2O yielding monolayers of 1T-MoS_2. In this case, we have demonstrated facile access to reduced and negatively charged 2H-MoS_2 with the retention of the semiconducting properties rather than conversion to a metallic nanomaterial as previously observed. The 2H-phase displays more promise for the development of electronic and optical devices, while the 1T- tends to be less desirable because of the high degree of defects and its metallic character. Until now, most protocols for the preparation of chemically derived TMDs like MoS_2 have yielded the 1T polytype. We anticipate chemical derivation of pre-exfoliated TMDs should open new avenues for further chemical derivation, facile dispersion in aqueous media, and novel applications of semi-conducting TMDs.

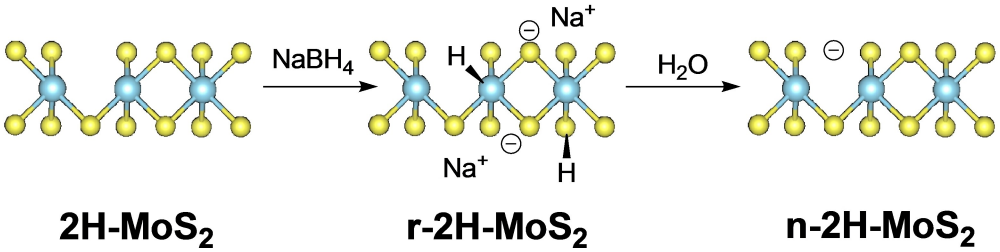

Scheme 2. Preparation of r- and n-2H-MoS_2.

Acknowledgements

This publication has emanated from research conducted with the financial support of Science Foundation Ireland (SFI), Grant Numbers SFI/12/RC/2278 2 and SFI/15/RS-URF/3307 and is co-funded under the European Regional Development Fund under the AMBER award. Open Access funding provided by IReL.

Conflict of Interests

The authors declare no conflict of interest.

Data Availability Statement

The data that support the findings of this study are available from the corresponding author upon reasonable request.

[1] a) H. Li, J. Wu, Z. Yin, H. Zhang, *Acc. Chem. Res.* **2014**, *47*, 1067–1075; b) J.-O. Joswig, T. Lorenz, T. B. Wendumu, S. Gemming, G. Seifert, *Acc. Chem. Res.* **2015**, *48*, 48–55; c) R. Lv, J. A. Robinson, R. E. Schaak, D. Sun, Y. Sun, T. E. Mallouk, M. Terrones, *Acc. Chem. Res.* **2015**, *48*, 56–64; d) H. Wang, C. Li, P. Fang, Z. Zhang, J. Z. Zhang, *Chem. Soc. Rev.* **2018**, *47*, 6101–6127.

[2] a) J. N. Coleman, M. Lotya, A. O'Neill, S. D. Bergin, P. J. King, U. Khan, K. Young, A. Gaucher, S. De, R. J. Smith, I. V. Shvets, S. K. Arora, G. Stanton, H. Y. Kim, K. Lee, G. T. Kim, G. S. Duesberg, T. Hallam, J. J. Boland, J. J. Wang, J. F. Donegan, J. C. Grunlan, G. Moriarty, A. Shmeliov, R. J. Nicholls, J. M. Perkins, E. M. Grieveson, K. Theuwissen, D. W. McComb, P. D. Nellist, V. Nicolosi, *Science* **2011**, *331*, 568–571; b) H. Li, Z. Yin, Q. He, H. Li, X. Huang, G. Lu, D. W. Fam, A. I. Tok, Q. Zhang, H. Zhang, *Small* **2012**, *8*, 63–67; c) Y. Zhan, Z. Liu, S. Najmaei, P. M. Ajayan, J. Lou, *Small* **2012**, *8*, 966–971; d) M. Chhowalla, H. S. Shin, G. Eda, L. J. Li, K. P. Loh, H. Zhang, *Nat. Chem.* **2013**, *5*, 263–275; e) M. O'Brien, N. McEvoy, T. Hallam, H. Y. Kim, N. C. Berner, D. Hanlon, K. Lee, J. N. Coleman, G. S. Duesberg, *Sci. Rep.* **2014**, *4*, 7374; f) C. Yim, M. O'Brien, N. McEvoy, S. Riazimehr, H. Schafer-Eberwein, A. Bablich, R. Pawar, G. Iannaccone, C. Downing, G. Fiori, M. C. Lemme, G. S. Duesberg, *Sci. Rep.* **2014**, *4*, 5458.

[3] a) G. Eda, H. Yamaguchi, D. Voiry, T. Fujita, M. Chen, M. Chhowalla, *Nano Lett.* **2011**, *11*, 5111–5116; b) A. Splendiani, L. Sun, Y. Zhang, T. Li, J. Kim, C. Y. Chim, G. Galli, F. Wang, *Nano Lett.* **2010**, *10*, 1271–1275; c) K. F. Mak, C. Lee, J. Hone, J. Shan, T. F. Heinz, *Phys. Rev. Lett.* **2010**, *105*, 136805.

[4] P. Joensen, R. F. Frindt, S. R. Morrison, *Mater. Res. Bull.* **1986**, *21*, 457–461.

[5] a) H. L. Tsai, J. Heising, J. L. Schindler, C. R. Kannewurf, M. G. Kanatzidis, *Chem. Mater.* **1997**, *9*, 879; b) D. Voiry, M. Salehi, R. Silva, T. Fujita, M. Chen, T. Asefa, V. B. Shenoy, G. Eda, M. Chhowalla, *Nano Lett.* **2013**, *13*, 6222–6227; c) A. Ambrosi, Z. Sofer, M. Pumera, *Small* **2015**, *11*, 605–612; d) X. Fan, P. Xu, D. Zhou, Y. Sun, Y. C. Li, M. A. T. Nguyen, M. Terrones, T. E. Mallouk, *Nano Lett.* **2015**, *15*, 5956–5960.

[6] a) R. Schöllhorn, A. Weiss, *J. Less Common Met.* **1974**, *36*, 229–236; b) J. Zheng, H. Zhang, S. Dong, Y. Liu, C. T. Nai, H. S. Shin, H. Y. Jeong, B. Liu, K. P. Loh, *Nat. Commun.* **2014**, *5*, 2995.

[7] a) W.-J. Xie, X. Li, F.-J. Zhang, *Chem. Phys. Lett.* **2020**, *746*, 137276; b) J. Zhang, Y. Wang, J. Cui, J. Wu, Y. Li, T. Zhu, H. Kang, J. Yang, J. Sun, Y. Qin, Y. Zhang, P. M. Ajayan, Y. Wu, *J. Phys. Chem. Lett.* **2019**, *10*, 3282–3289.

[8] a) C. Backes, N. C. Berner, X. Chen, P. Lafargue, P. LaPlace, M. Freeley, G. S. Duesberg, J. N. Coleman, A. R. McDonald, *Angew. Chem. Int. Ed. Engl.* **2015**, *54*, 2638–2642; b) A. M. Krajewska, A. E. Paiva, M. Morris, A. R. McDonald, *Chemistry (Weinheim an der Bergstrasse, Germany)* **2023**, *29*, e202302039.

[9] a) X. Chen, N. C. Berner, C. Backes, G. S. Duesberg, A. R. McDonald, *Angew. Chem. Int. Ed. Engl.* **2016**, *55*, 5803–5808; b) X. Chen, A. R. McDonald, *Adv. Mater.* **2016**, *28*, 5738–5746.

[10] S. Mouri, Y. Miyauchi, K. Matsuda, *Nano Lett.* **2013**, *13*, 5944–5948.

[11] M. Placidi, M. Dimitrievska, V. Izquierdo-Roca, X. Fontané, A. Castellanos-Gomez, A. Pérez-Tomás, N. Mestres, M. Espindola-Rodriguez, S. López-Marino, M. Neuschitzer, V. Bermudez, A. Yaremko, A. Pérez-Rodríguez, *2D Mater.* **2015**, *2*, 35006–35006.

[12] a) K. C. Knirsch, N. C. Berner, H. C. Nerl, C. S. Cucinotta, Z. Gholamvand, N. McEvoy, Z. Wang, I. Abramovic, P. Vecera, M. Halik, S. Sanvito, G. S. Duesberg, V. Nicolosi, F. Hauke, A. Hirsch, J. N. Coleman, C. Backes, *ACS Nano* **2015**, *9*, 6018–6030; b) É. Blanco, P. Afanasiev, G. Berhault, D. Uzio, S. Loridant, *C. R. Chim.* **2016**, *19*, 1310–1314.

[13] a) S. Mignuzzi, A. J. Pollard, N. Bonini, B. Brennan, I. S. Gilmore, M. A. Pimenta, D. Richards, D. Roy, *Phys. Rev. B* **2015**, *91*, 195411–195411; b) H. Guo, Y. M. Sun, P. F. Zhai, J. Zeng, S. X. Zhang, P. P. Hu, H. J. Yao, J. L. Duan, M. D. Hou, J. Liu, *Nucl. Instrum. Methods Phys. Res. Sect. B* **2016**, *381*, 1–5; c) B. R. Carvalho, Y. Wang, S. Mignuzzi, D. Roy, M. Terrones, C. Fantini, V. H. Crespi, L. M. Malard, M. A. Pimenta, *Nat. Commun.* **2017**, *8*, 14670; d) R. G. Costa, A. D. N. Barbosa, M. E. H. Maia da Costa, F. L. Freire, *Vib. Spectrosc.* **2022**, *123*, 103454–103454.

[14] A. M. Stacy, D. T. Hodul, *J. Phys. Chem. Solids* **1985**, *46*, 405–409.

[15] Y. Kang, S. Najmaei, Z. Liu, Y. Bao, Y. Wang, X. Zhu, N. J. Halas, P. Nordlander, P. M. Ajayan, J. Lou, Z. Fang, *Adv. Mater.* **2014**, *26*, 6467–6471.

[16] S. Jimenez Sandoval, D. Yang, R. F. Frindt, J. C. Irwin, *Phys. Rev. B Condens. Matter* **1991**, *44*, 3955–3962.

[17] X. Chen, P. Denninger, T. Stimpel-Lindner, E. Spiecker, G. S. Duesberg, C. Backes, K. C. Knirsch, A. Hirsch, *Chemistry (Weinheim an der Bergstrasse, Germany)* **2020**, *26*, 6535–6544.

[18] L. Nurdiwijayanto, R. Ma, N. Sakai, T. Sasaki, *Inorg. Chem.* **2017**, *56*, 7620–7623.

[19] D. Voiry, A. Goswami, R. Kappera, *Nat. Chem.* **2015**, *7*, 45–49.

[20] a) J. A. Schreifels, P. C. Maybury, W. E. Swartz, *J. Catal.* **1980**, *65*, 195–206; b) D. J. Joyner, D. M. Hercules, *J. Chem. Phys.* **1980**, *72*, 1095–1108.

[21] a) J. C. Dupin, D. Gonbeau, P. Vinatier, A. Levasseur, *Phys. Chem. Chem. Phys.* **2000**, *2*, 1319–1324; b) C. Andrello, T. Gouder, L. Favergeon, L. Desgranges, E. Tereshina-Chitrova, L. Havela, R. J. M. Konings, R. Eloirdi, *J. Nucl. Mater.* **2021**, *545*, 152646–152646.

[22] a) P. D. Schulze, S. L. Shaffer, R. L. Hance, D. L. Utley, *J. Vac. Sci. Technol. A-Vac. Surf. Films* **1983**, *1*, 97–99; b) J. Russat, *Surf. Interface Anal.* **1988**, *11*, 414–420.

[23] V. Cholet, L. Vandenbulcke, J. P. Rouan, P. Baillif, R. Erre, *J. Mater. Sci.* **2004**, *29*, 1417–1435.

[24] G. Berhault, L. C. Araiza, A. D. Moller, A. Mehta, R. R. Chianelli, *Catal. Lett.* **2002**, *78*, 81–90.

[25] N. Goel, N. Sinha, B. Kumar, *Mater. Res. Bull.* **2013**, *48*, 1632–1636.

[26] Q. Li, Y. Zhao, C. Ling, S. Yuan, Q. Chen, J. Wang, *Angew. Chem. Int. Ed. Engl.* **2017**, *56*, 10501–10505.

[27] a) H. G. Cho, L. Andrews, *J. Am. Chem. Soc.* **2005**, *127*, 8226–8231; b) S. Zhang, R. M. Bullock, *Inorg. Chem.* **2015**, *54*, 6397–6409.

[28] a) J. S. Kim, H. W. Yoo, H. O. Choi, H. T. Jung, *Nano Lett.* **2014**, *14*, 5941–5947; b) X. Chen, C. McGlynn, A. R. McDonald, *Chem. Mater.* **2018**, *30*, 6978–6982; c) M. D. Pluth, Z. J. Tonzetich, *Chem. Soc. Rev.* **2020**, *49*, 4070–4134.

[29] a) I. Wacławska, *J. Therm. Anal. Calorim.* **1998**, *53*, 519–532; b) Z. K. Peng, Q. M. Peng, Y. Q. Ma, *Ore Geol. Rev.* **2022**, *145*, 104887–104887.

[30] F. Ito, *Chem. Phys. Lett.* **2007**, *436*, 335–340.

[31] Y. Wang, K. Wang, C. Zhang, J. Zhu, J. Xu, T. Liu, *Small* **2019**, *15*, e1903816.

[32] a) K. E. Dungey, M. D. Curtis, J. E. Penner-Hahn, *Chem. Mater.* **1998**, *10*, 2152–2161; b) M. Acerce, D. Voiry, M. Chhowalla, *Nat. Nanotechnol.* **2015**, *10*, 313–318.

Manuscript received: June 5, 2024
Accepted manuscript online: June 6, 2024
Version of record online: August 19, 2024